

SYNCHROTRON RADIATION DISTRIBUTION AND RELATED OUTGASSING AND PRESSURE PROFILES FOR THE HL-LHC FINAL FOCUS MAGNETS*

R. Kersevan, CERN, Geneva, Switzerland

Abstract

The HL-LHC upgrade consists of many different subprojects. One of the most important ones is the installation of very large gradient inner triplet (IT) magnets, comprising 4 long superconducting (SC) quadrupoles, and a new superconducting D1 hosting a corrector package in the same cryostat. D2 is also a newly conceived SC magnet, and provision is made for 4x crab-cavities on each of the two separate beam lines, between D2 and Q4.

The HL-LHC final focus area, from Q4 to the interaction point, has been modelled based on the latest vacuum chamber geometry and orbits. The synchrotron radiation (SR) fans are computed using the Monte Carlo code SYNRAD+ [1]. The angular and energy dependence of the reflectivity of the copper surfaces is considered, as well as a representative surface roughness. Once the SR distributions are computed, they are converted into outgassing profiles by using conversion curves found in literature. The test-particle Monte Carlo code Molflow+ is then used [2] to compute the related gas density distribution. Warm areas are supposed to be NEG-coated, in order to reduce SR-induced desorption and the generation of secondary electrons. The calculation is repeated for 3 different conditioning times, corresponding to 1, 10, and 100 days at full nominal current of 1 A. It is shown that the resultant gas densities are always below the limit dictated by the ATLAS and CMS detectors' background and by the beam-gas scattering lifetime τ in the machine ($\tau > 100$ h). The SR ray-tracing calculations are carried out in the short-dipole approximation, i.e. no provision is made for edge radiation.

GEOMETRICAL ASSUMPTIONS

The latest geometry for the octagonal beam screen with tungsten-based shielding has been considered [3]. For the recombination chamber between D1 and TAN a "Y" chamber is assumed, with a common part for the two beams modelled as a 230 mm internal diameter (ID) round pipe splitting into two 80 mm ID separate chambers for the two beams. This "Y" chamber is supposed to be at room temperature, and NEG-coated, as presently done in the LHC. Since the exact geometry of the cold and warm beam-position monitors (BPMs) has not been finalized yet, they have been modelled as circular cylindrical objects connected to the neighbouring chambers via small-angle tapers. The cylindrical surface where the BPM electrodes are supposed to be located has a slightly bigger radius, so as to recess the electrodes and prevent them from being hit by direct SR coming from

the triplet area magnets. A similar model has been assumed for the RF contact fingers of the sliding joints placed in the inter-connects between the different cryostats and/or room-temperature vacuum chambers.

SYNCHROTRON RADIATION RAY- TRACING

The orbits for round beams at collision on the right side of IR1/IR5 have been considered [4]. It is against these orbits that the ray-tracing code SYNRAD+ has been checked prior to generating the detailed 3D model of the internal part of the perforated beam-screen (BS) and vacuum chambers. To this aim, the corresponding twiss file has been used, setting the initial point of each trajectory segment and the corresponding angles in SYNRAD+ to the same values as in the orbit file. For clarity, the case of the vertical crossing in IR1 has been chosen. Figure 1 shows the 8 different orbit segments in Q1, Q2a, Q2b, Q3, D1 and D2 (where Q1 and Q3 are in effect 2 shorter quadrupoles sitting inside the same cryostat, while Q2a and Q2b have separated cryostats with additional corrector packages). Initially the complete SR fan is collected separately for the outgoing B1 beam and incoming B2 beam on two large planar rectangular facets which allow us to calculate the global SR photon flux, power, and spectra, see Fig. 1. It has been decided to set a low-energy photon cut-off value of 4 eV, since neither molecular desorption nor photo-electron production is expected to be generated by photons having energies lower than this value. The MC code automatically calculates the fraction f of photons generated within the 4-500 eV energy interval. The critical energy for the SC magnets D1 and D2 is equal to 29.4 eV and 23.6 eV respectively, while the critical energy of the 4 SC triplet magnets depends on the distance between the orbit and the magnetic centre of the particular magnet. The fraction f is, 0.116, 0.152, 0.229, 0.237, 0.187, 0.171, for Q1a, Q1b, Q2a, Q2b, Q3a, and Q3b, respectively. This shows that only a small fraction of the photon flux calculated analytically is actually a potential source of molecules or photo-electrons, and that using the analytic formula which gives the number of photons emitted per unit length of trajectory largely overestimates the flux and the related photo-desorption and photo-electron production.

The beam size at each point of the orbit is calculated by taking into account the beam emittance, horizontal and vertical beta function, and dispersion as per standard formulae. Figure 1 shows in blue the cloud of source points of the SR rays traced. The local angle of emission is obtained by combining the natural SR divergence and

* Research supported by the High Luminosity LHC project

Content from this work may be used under the terms of the CC BY 3.0 licence © 2015. Any distribution of this work must maintain attribution to the author(s), title of the work, publisher, and DOI.

the additional angular spread generated by the lattice functions [5]. Table 1 summarizes the flux and power generated by each IT magnet, for the chosen orbit file:

Table 1: Photon Flux and Power (B1 / B2)

Magnet	Flux (ph/s)x10 ¹⁵	Power (W)
Q1a	9.04 / 10.1	0.0115 / 0.0132
Q1b	17.2 / 10.6	0.025 / 0.0140
Q2a	69.0 / 19.0	0.124 / 0.0257
Q2b	75.3 / 32.1	0.139 / 0.0482
Q3a	25.9 / 41.0	0.0414 / 0.0737
Q3b	21.2 / 47.3	0.0321 / 0.0887
D1	308 / 308	0.997 / 0.997
D2	279 / 279	0.788 / 0.788
SUM	805 / 747	2.158 / 2.049

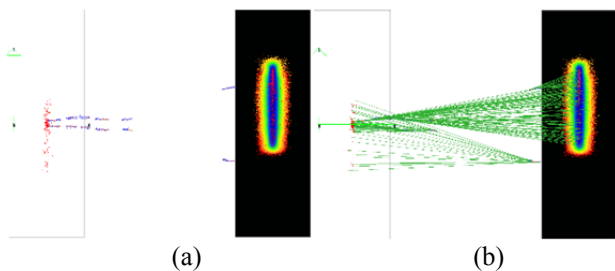


Figure 1: (a) Orbits (brown), source points scattered with Gaussian-like beam size (blue), and photon flux distribution on a vertical plane hit by B1 outgoing SR fans generated in the IT, D1 and D2. For B2, right-to-left direction, only the impingement points on another vertical plane are shown (red). (b) Ray tracing for both beams.

These photon fluxes are relatively small in absolute terms, and are spread over large areas, see Fig. 2. This means that the instantaneous molecular desorption rate will be small, but at the same time it will condition slowly.

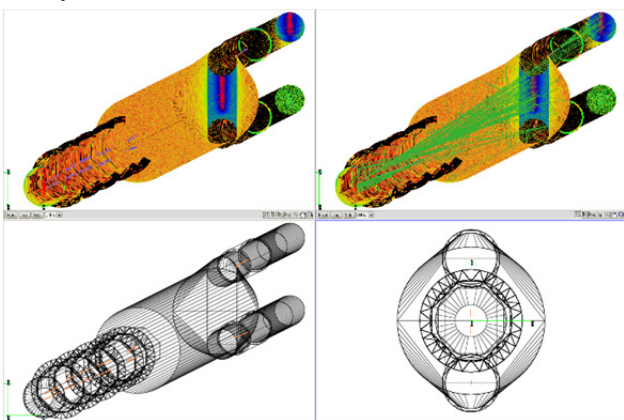


Figure 2: SYNRAD+ screenshot: ray tracing with modelled vacuum chamber geometry, TAS to Q4.

All surfaces are meshed with 1x1 cm² texture elements, except a few receiving higher photon flux densities were a finer 1x1 mm² texture size has been chosen. A total of about 1.6 million texture elements has been used. Each texture element keeps track of the photon flux density, power density, ray-traced hits, and absorbed rays. Each facet is also recording the global photon flux and power spectrum of the *absorbed* photons. The dependence of the reflectivity on the photon energy, angle of incidence, and surface roughness is taken into account (as explained in [1]).

It remains therefore to be seen whether the corresponding molecular density values are large as compared to the value of 10¹⁵ H₂ molecules/m³ which gives an acceptably small contribution to the local beam losses and beam-gas scattering lifetime reduction ($\tau > 100$ h), see [6].

MOLECULAR FLOW SIMULATIONS

Once the SR ray-tracing code SYNRAD+ is run for a sufficiently long time, in order to smooth out the statistical fluctuations especially on low-flux surfaces, it is the turn of the molecular flow MC code Molflow+. The photon flux on each texture element of the simulation is weighted and converted into a corresponding outgassing load by applying known photon-to-molecule conversion values found in literature, as a function of the various materials, temperatures and the machine conditioning time. The photon flux impinging the TAS entrance, and the 2 Q4 openings are supposed not to generate any gas load inside this model.

Temperatures

In a non-isothermal vacuum system like the one we are describing here, the concept of pressure can generate misleading results. It is better to use the molecular density, which can be easily related to the beam-gas scattering lifetime of the stored proton beams [6]. Since the photo-desorption yield data at very low temperatures are scarce, we have numerically extrapolated data obtained at LN₂ or room temperature. It has been assumed that the BSs of the triplet and D1 magnet are kept at a temperature of 50 K, while the BPM and RF-contact fingers are floating at a slightly higher temperature of 75 K (no direct cooling loop on them). The octagonal BS of the D2 magnet has been assumed to be at 15 K (no collision debris on it, see [7]). The exact geometry of the crab cavities has not been modelled: a circular pipe of 80 mm ID at 2 K has been assumed to be placed along the length reserved for such cavities. Also, details of the aperture restrictions and geometries of fixed or moveable collimators have not been integrated into this model yet.

Molecular Sticking Coefficients

For the time being, only the behaviour of H₂ has been modelled, since it is known from LHC operation to constitute the major part of the gas load. The following

sticking coefficients have been applied to those facets which have a pumping action on H₂, as follows:

- A sticking coefficient $s=1$ on all surfaces below 4.5 K.
- $s=0$ on all surfaces above 4.5 K.
- $s=0.008$ for all room-temperature, NEG-coated surfaces
- $s=0.8$ at the circular opening modelling the entrance of the Q4 quadrupole (both B1 and B2 beam lines)
- A sticking of 0.406 has been assumed on 4 rectangular facets of 19.35 cm² surface each in order to model an effective pumping speed for H₂ of 700 l/s between the TAS and Q1a. The relationship between s and the corresponding pumping speed S (l/s) is given by the simple formula

$$S(l/s) = \frac{1}{10} \sqrt{\frac{R \cdot T}{2 \cdot \pi \cdot M}} \cdot A \cdot s \quad (1)$$

where A is the area in cm² of the facet having sticking s ; R is the gas constant, 8.3145 J/K; M is the molar mass in kg/mole; the square root factor is 1/4 the average speed of the gas of molecular mass M and temperature T , in m/s; 1/10 is a conversion factor accounting for the units (l/s instead of m³/s, and cm² instead of m²).

- Along 4 of the 8 facets of each BS (those inclined at ± 45 degrees with respect to the vertical plane) a sticking coefficient s has been assigned so as to simulate the pumping speed given by the 4 rows of racetrack-shaped slots (0.8mm x 8 mm average length, 1 mm thick). Once a molecule has gone through a slot, it is efficiently pumped by the 2 K cold bore of the superconducting magnets. The transmission probability of the average slot has been calculated separately, P_{tr} , and then the total surface of the slots for each BS facet has been obtained by multiplying the area of the average slot times 235.5, the latter being the average number of slots per meter of length of each BS facet. This has then been multiplied by the length L (m) of each BS, and also by P_{tr} . Summarizing, the *equivalent* sticking coefficient of each slotted BS facet of area A (cm²) has been calculated as:

$$s = 1 - (A - 235.5 \cdot L \cdot P_{tr}) / A \quad (2)$$

The saturation of the NEG-coated surfaces has not been taken into account, and that is why a rather conservative value of 0.008 for H₂ has been chosen.

Figure 3 shows the H₂ density for the B1 beam (outgoing) for 3 different values of the accumulated beam dose.

Electron Cloud and Ion Bombardment Effects

For the time being, no e-cloud source of pressure rise has been considered: the HL-LHC project assumes a baseline of no e-cloud, meaning that appropriate materials and/or surface treatments will be developed and applied so that e-cloud cannot take place (see for instance [8], this conference). A similar assumption has been made concerning the ion-bombardment, it has assumed to be absent. The results of these calculations will be used to ascertain whether areas of high-pressure, and potential interaction with the beam and its subsequent ionization, could potentially be present.

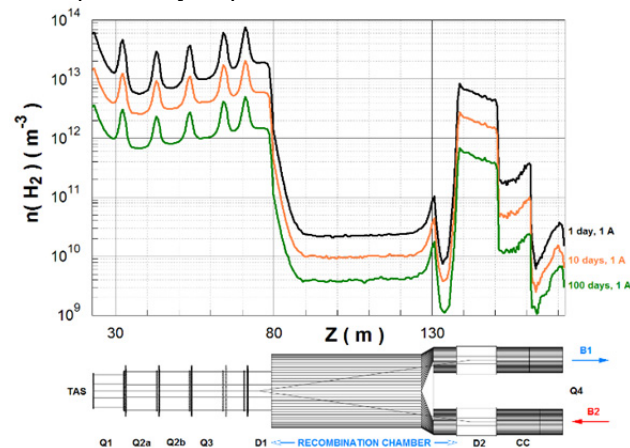


Figure 3: H₂ density profiles for 24, 240, and 2400 A.h.

FUTURE WORK

As the HL-LHC project matures and the details of all components of the IT area which have not been finalized yet become available to us, the 3D models will be modified and the two MC codes run again. The contribution of other gas species, and the simulation of leaks, will also have to be carried out. A similar analysis is being carried out in parallel on the more demanding FCC-hh design study, where SR is expected to play a much bigger role than in the LHC and HL-LHC upgrade [9, 10].

CONCLUSIONS

We have shown that under reasonable assumptions about the materials, geometry and outgassing of the IT magnet area, the HL-LHC upgrade of IR1 and IR5 should not face synchrotron radiation-related high residual-gas density levels incompatible with the energy deposition in the detectors' areas or beam-gas scattering lifetime of the rings. As the design of components such as the crab cavities, BPMs, etc... advances, new calculations will be carried out, and any potential show stoppers spotted and dealt with.

ACKNOWLEDGEMENTS

R. de Maria, CERN/BE-ABP-HSS, is gratefully acknowledged for providing advice on the orbit plots and files; C. Garion and V. Baglin, CERN/VSC, for useful

comments and clarifications; R. Menendez, CERN/EN-MEF-QOP, for providing the geometry of the beam-screen in the triplets; M. Ady, CERN/VCS, for developing the 2 MC codes.

REFERENCES

- [1] SYNRAD+ website:
<http://test-molflow.web.cern.ch/content/synrad-documentation>
- [2] Molflow+ website: <http://cern.ch/test-molflow>
- [3] C. Garion et al., “Preliminary Design of the High-Luminosity LHC Shielded Beam Screen”, MOBD1, these proceedings, IPAC’15, Richmond, USA (2015).
- [4] R. de Maria, http://lhc-optics.web.cern.ch/lhc-optics/www/hllhc11/round/twiss_irlb1.csv
- [5] G. K. Green, “Spectra and optics of synchrotron radiation”, BNL Note BNL50522, April 1976; <http://www.bnl.gov/isd/documents/20484.pdf>
- [6] O. Bruning et al., “LHC Design Report, Vol.1”, (2004).
- [7] F. Cerutti, F. Esposito, “Collision Debris in the TAS-Triplet-D1 Region”, 4th Joint HiLumi LHC-LARP Meeting, KEK Laboratory, Japan (2014), <http://indico.cern.ch/event/326148/session/17/contribution/42/material/slides/1.pdf>
- [8] R. Salemme et al., “Amorphous Carbon Coatings at Cryogenic Temperatures with LHC Nominal Beams: First Results with the COLDEX Experiment”, WEPHA007, these proceedings, IPAC’15, Richmond, USA (2015).
- [9] R. Kersevan, “Synchrotron Radiation and Vacuum Concepts”, FCC Kick-Off Meeting, University of Geneva, Switzerland (2014); <https://indico.cern.ch/event/282344/session/2/contribution/25>
- [10] C. Garion, “Arc Vacuum Considerations and Beam Screen Design”, FCC Week 2015, Marriott Hotel Georgetown, Washington D.C., USA (2015); <http://indico.cern.ch/event/340703/session/71/contribution/106/material/slides/1.pdf>